Applied Surface Science 311 (2014) 870–875

Contents lists available at ScienceDirect

Applied Surface Science

journal homepage: www.elsevier.com/locate/apsusc

Optimization of shunt isolation processing for silicon solar cells via laser and chemical etching

H.L. Hao[a,*], S.H. Zhong[b], X. Zhang[a], W.Z. Shen[b]

[a] College of Material Engineering, Shanghai University of Engineering Science, 333 Long Teng Road, Shanghai 201620, China
[b] Institute of Solar Energy, and Key Laboratory of Artificial Structures and Quantum Control (Ministry of Education), Department of Physics and Astronomy, Shanghai Jiao Tong University, 800 Dong Chuan Road, Shanghai 200240, China

ARTICLE INFO

Article history:
Received 2 December 2013
Received in revised form 24 March 2014
Accepted 7 May 2014
Available online 2 June 2014

Keywords:
Silicon solar cell
Shunt isolation
Laser scribing
Chemical etching

ABSTRACT

We employ laser scribing combined with chemical etching process to isolate the shunts in industrial off-spec or non-prime crystalline solar cells. Liquid crystal sheet and Infrared camera measurements have been carried out to reveal the existence of the shunts and hot spot temperature under reverse bias. Following laser scribing with proper laser parameters, chemical etching has been used to further optimize the isolation effect. Through illuminated current–voltage characteristic measurements, the improved open circuit voltage, fill factor and efficiency have been obtained. These results demonstrate that this combined shunt isolation process has great potential for its application in the solar cells.

© 2014 Elsevier B.V. All rights reserved.

1. Introduction

With the extensive application of solar power produced by crystalline silicon solar modules, a significant percentage of solar cells are classified as off-spec or non-prime cells as a result of electrical shunts. Usually, the electrical shunts will act to electrically by-pass the devices internal p-n junction within the crystalline silicon solar cells. In this paper, all the bright features visible in liquid crystal sheet (LC) or infrared (IR) camera measurement have been called "shunts", which are caused by material or process. Several types of shunts have been found and classified into the following types: linear/nonlinear edge shunts, cracks and holes, Schottky-type shunts, etc. [1]. Shunts can be presented in different localized regions in solar cells, which will decrease the cell conversion efficiency (η) under forward bias by decreasing short circuit current and fill factor (*FF*). Meanwhile, the shunt in a solar cell will result in "hot spot" formation under reverse bias conditions, which is due to the local dissipation of power through the shunt, and the hot spot temperature relates to the local reverse current density [2]. If the temperature generated by the shunt exceeds a critical value, the solar module in which the cells are integrated can be damaged. According to IEC qualification testing procedure for hot spot testing at module level, a module should be maintained at a temperature of $50 \pm 10\,^{\circ}C$ during a five hours exposure in simulated or nature sunlight with an irradiance of $1000\,W/cm^2 \pm 10\%$ [3]. Therefore, it is a major challenge facing PV manufactures to minimize the shunt influence on silicon solar cells.

Traditionally, the shunted silicon-based cells are discarded, or disposed by chemical solutions and then re-undergo the fabrication process, during which metal contamination is hard to get rid of, and the reprocessed wafers become very thin, thus making handling operation and screen-printing difficult. As a result, more effective methods are needed to repair shunted areas. By isolating the shunted regions from the active areas, a non-prime cell will be possibly up-graded, which can be accomplished by either physically removing the shunt itself or by eliminating the conductive paths connecting the shunt to the rest of the cell [2,4–9].

Up to now, laser scribing is widely used to isolate shunts, it is perfectly suitable for inline processing and the solar cells needs not to be touched, which is an important to handle thin wafers. However, due to the recast of molten or new shunts induced by the laser scribing, the reported results cannot be satisfied. In this paper, by adopting chemical etching after laser scribing, we can further improve the laser scribing isolation effect, and the enhanced cell efficiency could be expected.

2. Experimental details

The studied multi-crystalline solar cells with dimension of $156 \times 156\,mm^2$ were named by *Sx* ($x = 1, 2, 3, 4$), all of them were

* Corresponding author. Tel.: +86 21 67791474.
E-mail address: huilian.hao@sues.edu.cn (H.L. Hao).

http://dx.doi.org/10.1016/j.apsusc.2014.05.078
0169-4332/© 2014 Elsevier B.V. All rights reserved.

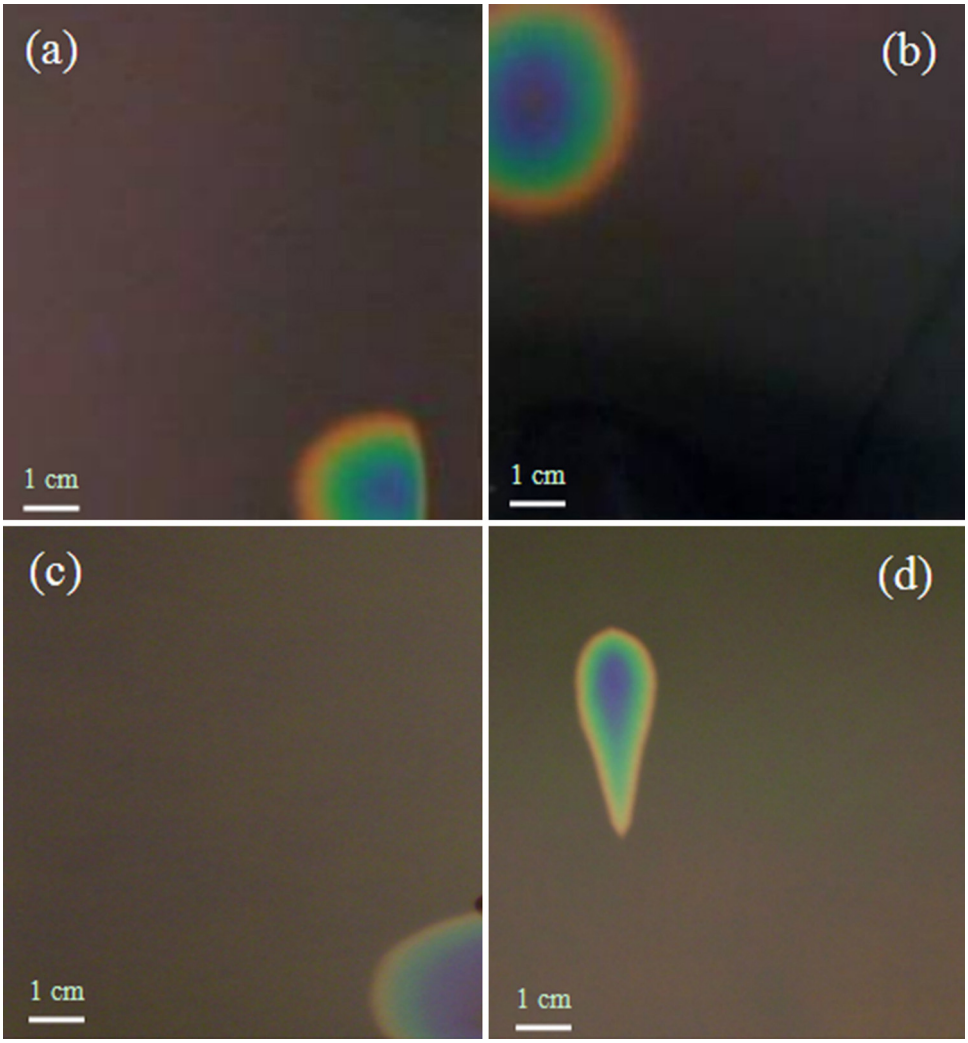

Fig. 1. Liquid crystal images (a), (b), (c), (d) under reverse bias 10 V, corresponding to the samples of S1, S2, S3, S4, respectively. (For interpretation of the references to color in text, the reader is referred to the web version of the article.)

fabricated from p-type wafers with conventional structure of front junction and back surface fields: Ag/n^+–Si/p–Si/P^+–Si/Al. Due to the lower efficiencies than those of the normal products, all of them were rejected by the manufacture. LC measurement was performed under reverse bias to detect the shunts in the samples. The 1064 nm Q-switched Nd:YAG pulsed laser was used to isolate shunted areas within the cells. Profiler meter (NT9080) measurement with 20× objective was carried out to characterize the depth and width of the scribing groove. After laser scribing, the electrochemical etching was implemented with 12% NaOH solution. An IR camera with FLIR systems was used to measure the hot spot temperature (T_h) at reverse bias of 10 V. Finally, illuminated current–voltage (*I–V*) characterization was carried out under standard conditions (under AM 1.5 G illumination at 25 °C) with a Gsolar XJCM-9 *I–V* tester to characterize the electrical properties of all the samples.

3. Results and discussion

We firstly employ LC sheets measurement to detect the shunts in the samples. The LC sheet containing a thermo chromic LC layer film is about 160 μm thick with the sensitive temperature range of 25–30 °C, the color of which will change when the temperature rises in shunt positions under a reverse bias. Note that the visual appearance of hot spots in LC sheet imaging strongly depends on the heating power and measuring time on the solar cells. Fig. 1 gives the LC imaging of the samples under reverse bias 10 V. During the LC measurement, the temperature of shunt increases with test time under a certain voltage, thus the color scale of LC sheet around shunt region goes from black across red, yellow, green to blue. The blue color represents the highest temperature, and then instantly dark dip appears inside the blue region, which displays the shunt position [10]. We can see from Fig. 1 that the shunts are lying in different positions in different samples, three of them locate on the edge of the solar cells, indicating that the edge of the solar cells were not well-passivated. It is clear that the color regions are much larger in S1 and S2 than those in S3 and S4, which means that shunts in S1 and S2 are much stronger than those in S3 and S4.

In order to upgrade these samples, the shunt isolation was performed by laser scribing to eliminate the conductive paths connecting the shunt to the rest of the solar cell. Incorrect laser settings can result in the metal residues or other dirty stains going into the scribing grooves, especially when the laser scribes cross a contact finger. As a result, these residues will produce very low resistive paths that easily cause shunts across the junction. To identify the suitable laser parameters for good shunt isolation, laser scribing was first performed on several non-shunted solar cells to obtain the optimized laser parameter. As confirmed by LC sheet and IR

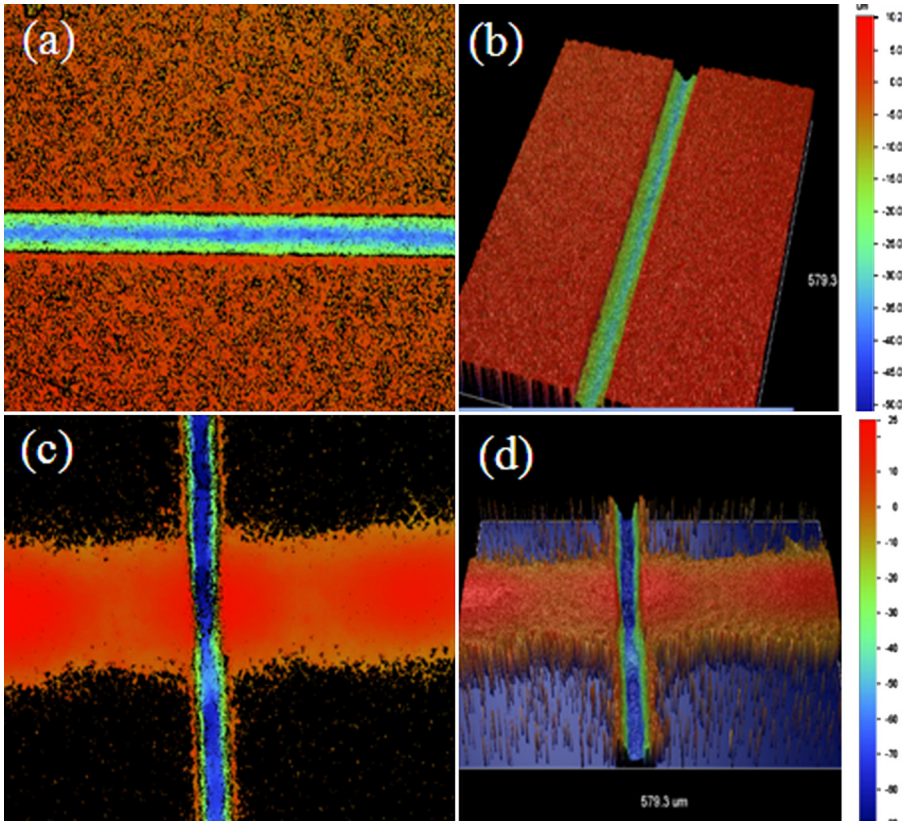

Fig. 2. Plan and corresponding 3-D profiles of the laser grooves by profiler meter measurements: in the areas of SiN-coated silicon (a) and (b), as well as gridlines (c) and (d).

camera measurements, the non-shunted solar cells before scribing had no localized shunts. Under reverse bias 10 V, the reverse current (I_{rev}) of all the cells was below 0.1 A. The deduced shunt resistances R_{sh}, which are referred as the leakage path of the current in a solar cell and represented in parallel with the current source in equivalent circuit model [11], were larger than 100 Ω. The scribing processes were done with Q-switched (nanoseconds) Nd:YAG pulsed laser pumped by the krypton light. The effects of laser parameters (laser average power-$P_{average}$, repetition rate-R_{rep}, scanning speed-$V_{scanning}$, pulse duration-W_{pulse}, spot size-D_{size} and loop count number) on the processed samples were evaluated by comparing the changes of shunt resistance and I_{sc} before and after laser scribing. The I–V testing was performed under standard condition for all the samples to get R_{sh} and I_{sc}. During the laser process on non-shunted cells, a square with size of 5 mm × 5 mm was scribed, which includes the contact finger. In the area of SiN-coated silicon, the laser groove width and depth are 50 and 32 μm, respectively. While in the area of gridlines, the laser groove width and depth are 35 and 26 μm, respectively. The R_{sh} for all non-shunted cells before and after laser scribing is 135.0–266.3 Ω and 128.6–251.3 Ω, respectively.

Note that the laser scribing groove depth should be much deeper than the thickness of gridlines to guarantee proper scribing through the gridlines, which is a balance between good isolation and strength properties. During our experiments, we found that the depth of the laser groove mainly depended on the scanning speed and pulse duration. A trade-off between the new shunts produced by the laser scribing and the suitable groove depth should be taken into account to obtain the smallest changes of R_{sh} and I_{sc}. For scribing in the middle and at the edge of the samples, we got the smallest I_{sc} loss around 1.4% and 0.6%, with R_{sh} decrement 15 Ω and 3 Ω, respectively. Then the above optimized corresponding laser settings were used to isolate the shunts. For the samples S1–S3, the laser parameters used are: $P_{average}$ (20 W), R_{rep} (30 KHz), $V_{scanning}$ (400 mm/s), W_{pulse} (175 ns) and D_{size} (20 μm). While for the sample S4, the laser parameters used are: $P_{average}$ (50 W), R_{rep} (50 KHz), $V_{scanning}$ (600 mm/s), W_{pulse} (256 ns) and D_{size} (30 μm). When scribing the shunted cells, the laser light firstly focused on the emitter surfaces and then scribed with double laser passes. The shunted areas were scribed by a square shape, until the shunted areas were electrically isolated from the rest of the cells. The square size is 5 mm × 5 mm, which can surround the shunted areas completely, the laser groove crosses through the contact fingers. The isolation grooves through emitter and through metal grid lines were formed by overlapping these pulses to produce a continuous groove, and the start-end point overlap is 65%. Finally, the depth and width measurements of the laser grooves were carried out at different locations.

Fig. 2 presents the plan and corresponding 3-D profiles of the laser grooves in the areas of SiN-coated silicon and gridlines by profiler meter measurements. Both the scribing depth and width were measured in 10 different places away from the gridlines and in 5 places where the scribe crossed a gridline. The laser groove width is ~48 μm in the area of SiN-coated silicon and 35 μm in that of gridlines, the corresponding groove depth is 32 μm and 25 μm, respectively. The ridges on each side of the scribe rose to a height about 10 μm above the mean surface level of the cell. The height of ridge can influence the scribing effect, low ridge will decrease the debris collapsing probability to form new shunts when handling the cells. Usually, the height of the gridlines was found to be 10–15 μm, so the laser scribing can completely disconnect the metal connecting the shunted area to the rest of the solar cells. We can see that all the laser grooves are quite clean, which indicates that laser scribing has been well implemented.

To further improve the isolation effect, electrochemical etching was carried out to etch print paste stains or other dirties induced

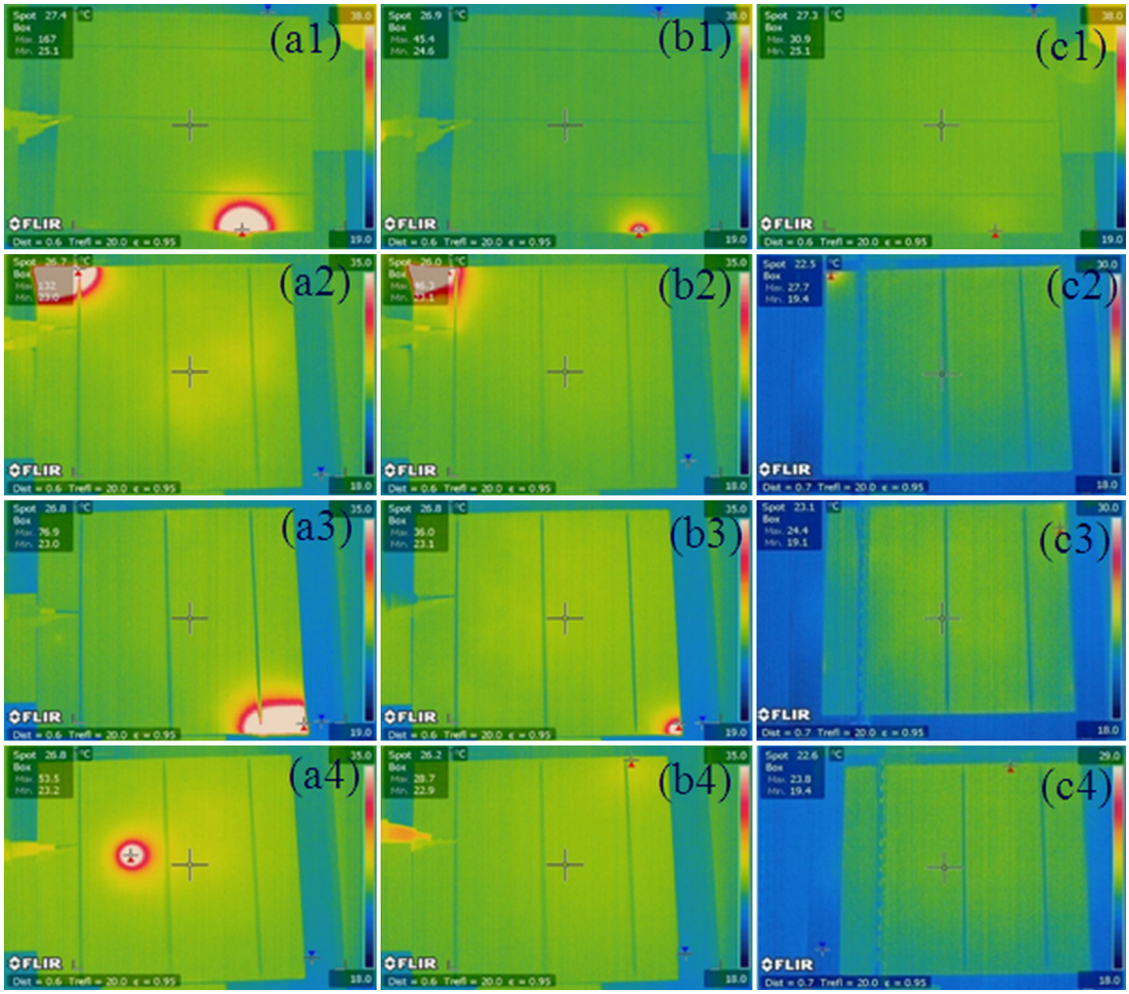

Fig. 3. IR images under reverse bias 10 V of all the samples: (a1)–(a4) before shunt isolation, (b1)–(b4) after laser scribing, and (c1)–(c4) after chemical etching.

by the laser scribing with 12% NaOH solution. The cell was laid on a copper plate and connected to a power supply by means of two handheld electrodes. Then, 12% NaOH was dropped inside the laser grooves. Under a bias voltage, the current started running through the cell, and some bubbles can be seen in the grooves during etching process, which indicates that some reactive chemical reactions occur there.

During the chemical etching, the print paste stains or other dirties (e.g. Al, SiO_2, SiC, etc.) induced by the laser scribing can be got rid of. The following electrochemical reactions can be expected to occur:

$$2Al + 2OH^- + 2H_2O \rightarrow 2AlO_2^- + 3H_2 \uparrow$$

$$SiC + 2OH^- + H_2O \rightarrow SiO_3^{2-} + CH_4 \uparrow$$

$$SiO_2 + 2OH^- \rightarrow SiO_3^{2-} + H_2O$$

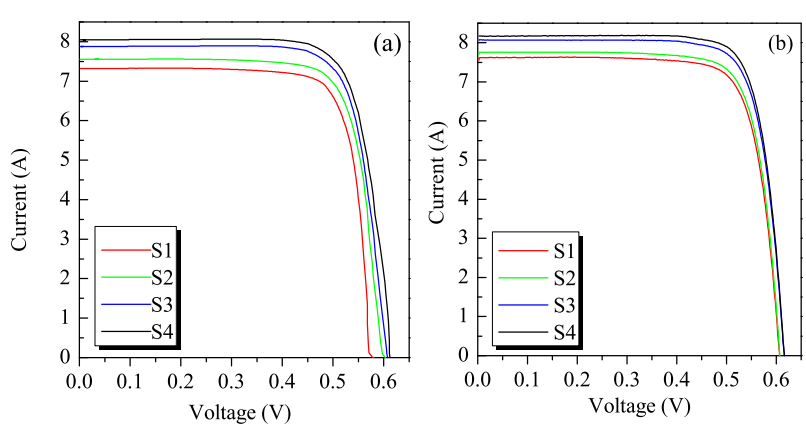

Fig. 4. Illuminated *I–V* characteristic curves of all the samples: (a) after laser scribing and (b) after etching.

Table 1
The hot spot temperature and reverse current at −10 V for all the samples before isolation, after laser scribing, and after etching.

Samples	Before isolation		After laser scribing		After etching	
	T (°C)	I_{rev} (A)	T (°C)	I_{rev} (A)	T (°C)	I_{rev} (A)
S1	167	7.50	45.4	0.46	30.2	0.37
S2	132	6.48	46.3	0.33	27.1	0.27
S3	76.9	4.33	36.0	0.26	26.5	0.02
S4	53.5	2.56	28.7	0.15	22.1	0.007

Table 2
Comparison of the electrical performance of all samples at various processing stages.

Samples	Before isolation				After laser scribing				After etching			
	V_{oc}(mV)	I_{sc}(A)	FF(%)	η(%)	V_{oc}(mV)	I_{sc}(A)	FF(%)	η(%)	V_{oc}(mV)	I_{sc}(A)	FF(%)	η(%)
S1	542.1	5.29	50.8	6.9	580.7	7.32	75.9	11.8	606.2	7.55	78.1	12.3
S2	554.9	5.71	55.2	7.5	602.9	7.55	78.4	13.8	606.1	7.70	80.8	14.1
S3	587.4	6.12	61.3	9.4	608.5	7.87	81.6	15.5	615.7	8.06	82.5	15.7
S4	591.1	7.25	68.5	10.4	612.9	8.04	82.1	16.1	615.9	8.17	82.8	16.3

The etching process was kept 5 min, and then the etch paste and reaction products were removed by rinsing the cell with deionized water. Finally, the ethanol was sprayed on the cells to avoid marks.

Through LC sheet experiment, the position of the shunts can be identified on the solar cells, while the temperature of hot spot cannot be determined under a reverse bias. The hot spots temperature is related to the local reverse current density, if the temperature generated by shunt is too high, the solar module in which the cell is integrated can be damaged. The temperature under a reverse bias can be determined by an IR measurement, which was carried out to obtain T_h under a reverse bias. Fig. 3 shows IR images under reverse bias 10 V of all the samples before isolation (a1–a4), after laser scribing (b1–b4), and after etching (c1–c4). It can be seen that the shunted areas (bright zones) lie on the edge and in the middle of the samples for S1–S3 and S4, respectively, which are consistent with those in Fig. 1. From IR images, T_h and I_{rev} at reverse bias 10 V can be read for all the samples at different process stages, all the measurements were under the same condition. For clarity, T_h and I_{rev} obtained from IR measurement under −10 V were summarized in Table 1. It is obvious that T_h and I_{rev} decrease significantly after laser scribing, moreover, further decrement can be still observed after electrochemical etching treatment, due to that the possible metal or small quantity of drains driven into the junction by laser were peeled off during the etching. The final I_{rev} is below 0.5 A for all the samples, and the deduced R_{sh} is larger than 20 Ω, which can completely meet the hot spot test that is routinely carried out on every cell by the manufactures.

Fig. 4 shows the illuminated I–V characteristic curves for the samples after laser scribing (Fig. 4(a)) and after etching (Fig. 4(b)), respectively. Some electrical data of all the samples determined from the illuminated I–V measurements are summarized in Table 2. The significant improvement in the electrical properties of the samples after etching demonstrates the potential of the proposed technique. The improvement in the electrical properties can be explained as the follows: the laser scribing removes shunted regions electrically from the main part of cell, thus the direct conductive paths from the emitter at shunted regions to the rear p-contact are eliminated. Therefore, a portion of the photo-generated current cannot directly flow through the emitter to the back contact but flow through the external circuit. According to two-diode equivalent circuit model [5], R_{sh} will increase due to the parasitic current path interrupted by the shunt isolation process, thus reduces the influence of the shunt on FF and open circuit voltage (V_{oc}), which also results in the isolated area no longer being able to contribute to the current [12]. Therefore, the increment in efficiency for all the samples can be obtained due to the increase of I_{sc}, V_{oc} and FF. After etching processes, the electrical properties are sustainably improved for all the samples, indicating that the etching can further optimize isolation effect through chemically treating the scribing grooves. All these results confirm that the localized shunts can be well isolated by a combination of laser scribing and chemical etching technique.

4. Conclusion

In summary, we employed LC sheet and IR camera to reveal the existence of the localized shunts, reverse current and hot spot temperature under a reverse bias. The optimized laser settings and chemical etching were applied to isolate the shunted regions in industrial off-spec solar cells. After shunts isolation, the electrical parameters (FF, I_{sc}, V_{oc}, η) of these samples obtained from illuminated I–V characteristic curves were recovered to the acceptable levels by the manufactures. It is shown that the localized shunt isolation through laser scribing combined with chemical etching can yield functional solar cells in terms of thermal and electrical properties, demonstrating the application prospect of the proposed isolation technique.

Acknowledgments

This work was supported by National Major Basic Research Project of 2012CB934302, the Research Fund for the Doctoral Program of Shanghai University of Engineering Science under contract 201308, Shanghai Youth College Teachers Training Program of ZZGJD13023, and Top Discipline Plan for Mechanical Engineering of Shanghai Municipal Education Commission (YLJX12-2).

References

[1] O. Breitenstein, J.P. Rakotoniaina, M.H. Al Rifai, M. Werner, Shunt types in crystalline silicon solar cells, Prog. Photovolt. Res. Appl. 12 (2004) 529–538.
[2] A.M. Petersson, D. Chithambaranadhan, Q. Nguyen, R. Goldberg, T. Lommasson, T. Boström, Shunt isolation in silicon solar cells by chemical etching, in: 25th EUPVSEC, Valencia, Spain, 2010.
[3] IEC 61215, Crystalline Silicon Terrestrial Photovoltaic Modules-Design Qualification and Type Approval, 1993.
[4] L.C. Zhang, H. Shen, Z.J. Yang, J.S. Jin, Shunt removal and patching for crystalline silicon solar cells using infrared imaging and laser cutting, Prog. Photovolt. Res. Appl. 18 (2010) 54–60.
[5] D. Kray, S. Hopmana, A. Spiegel, B. Richerzhagen, G.P. Willeke, Study on the edge isolation of industrial silicon solar cells with waterjet-guided laser, Sol. Energy Mater. Sol. Cells 91 (2007) 1638–1644.
[6] M.D. Abbott, T. Trupke, H.P. Hartmann, R. Gupta, O. Breitenstein, Laser isolation of shunted regions in industrial soalr cells, Prog. Photovolt. Res. Appl. 15 (7) (2007) 613–620.

[7] A. Hauser, G. Hahn, M. Spiegel, H. Feist, O. Breitenstein, J.P. Rakotoniaina, P. Fath, E. Bucher, Comparison of different techniques for edge isolation, in: 17th European Photovoltaic Solar Energy Conference and Exhibition, Munich, 2001, pp. 1–4.
[8] G. Emanuel, E. Schneiderlöchner, J. Stollhof, J. Gentischer, R. Preu, R. Lüdemann, High throughput laser isolation of crystalline silicon solar cells, in: Proceedings of the 17th European Photovoltaic Solar Energy Conference, Munich, 2001, pp. 1578–1581.
[9] I.M. Hamammu, K. Ibrahim, Solar cell edge shunt isolation: a simplified approach, Proc. ICSE 19–21 (2002) 230–232.
[10] O. Breitenstein, J.P. Rakotoniaina, J. Schmidt, Comparison of shunt imaging by liquid crystal sheets and lock-in thermography, in: Proceedings of the 12th Workshop on Crystalline Solar Cell Materials and Processes, Vol. 12, Breckenridge, CO 12, 2002, pp. 244–246.
[11] C.S. Solanki, Solar Photovoltaic: Fundamentals, Technologies and Applications, 2011, pp. 103.
[12] O. Breitenstein, M. Langenkamp, J.P. Rakotoniaina, The imaging of shunts in solar cells by infrared lock-in thermography, in: Proceedings of the 17th European Photovoltaic Solar Energy Conference, Munich, 2001, p. 1499.